

RESEARCH

Open Access



Varied cellular abnormalities in thin vs. normal endometrium in recurrent implantation failure by single-cell transcriptomics

Xiaoying Fu^{1†}, Xiaoyan Guo^{2†}, Han Xu^{1†}, Yini Li³, Bihui Jin¹, Xirong Zhang⁴, Chongyi Shu¹, Yuhang Fan¹, Yiqi Yu¹, Yuqing Tian¹, Jiao Tian² and Jing Shu^{1,2,5*}

Abstract

Background Reduced endometrium thickness and receptivity are two important reasons for recurrent implantation failure (RIF). In order to elucidate differences between these two types of endometrial defects in terms of molecular signatures, cellular interactions, and structural changes, we systematically investigated the single-cell transcriptomic atlas across three distinct groups: RIF patients with thin endometrium (≤ 6 mm, TE-RIF), RIF patients with normal endometrium thickness (≥ 8 mm, NE-RIF), and fertile individuals (Control).

Methods The late proliferative and mid-secretory phases of the endometrium were collected from three individuals in the TE-RIF group, two in the NE-RIF group, and three in the control group. The study employed a combination of advanced techniques. Single-cell RNA sequencing (scRNA-seq) was utilized to capture comprehensive transcriptomic profiles at the single-cell level, providing insights into gene expression patterns within specific cell types. Scanning and transmission electron microscopy were employed to visualize ultrastructural details of the endometrial tissue, while hematoxylin and eosin staining facilitated the examination of tissue morphology and cellular composition. Immunohistochemistry techniques were also applied to detect and localize specific protein markers relevant to endometrial receptivity and function.

Results Through comparative analysis of differentially expressed genes among these groups and KEGG pathway analysis, the TE-RIF group exhibited notable dysregulations in the TNF and MAPK signaling pathways, which are pivotal in stromal cell growth and endometrial receptivity. Conversely, in the NE-RIF group, disturbances in energy metabolism emerged as a primary contributor to reduced endometrial receptivity. Additionally, using CellPhoneDB for intercellular communication analysis revealed aberrant interactions between epithelial and stromal cells, impacting endometrial receptivity specifically in the TE-RIF group.

Conclusion Overall, our findings provide valuable insights into the heterogeneous molecular pathways and cellular interactions associated with RIF in different endometrial conditions. These insights may pave the way for targeted

[†]Xiaoying Fu, Xiaoyan Guo and Han Xu contributed equally to this work.

*Correspondence:
Jing Shu
shujing@hmc.edu.cn

Full list of author information is available at the end of the article



© The Author(s) 2024, corrected publication 2024. **Open Access** This article is licensed under a Creative Commons Attribution-NonCommercial-NoDerivatives 4.0 International License, which permits any non-commercial use, sharing, distribution and reproduction in any medium or format, as long as you give appropriate credit to the original author(s) and the source, provide a link to the Creative Commons licence, and indicate if you modified the licensed material. You do not have permission under this licence to share adapted material derived from this article or parts of it. The images or other third party material in this article are included in the article's Creative Commons licence, unless indicated otherwise in a credit line to the material. If material is not included in the article's Creative Commons licence and your intended use is not permitted by statutory regulation or exceeds the permitted use, you will need to obtain permission directly from the copyright holder. To view a copy of this licence, visit <http://creativecommons.org/licenses/by-nc-nd/4.0/>.

therapeutic interventions aimed at improving endometrial receptivity and enhancing reproductive outcomes in patients undergoing ART. Further research is warranted to validate these findings and translate them into clinical applications for personalized fertility treatments.

Trial registration Not applicable.

Keywords Single-cell sequencing, Thin endometrium, Recurrent implantation failure

Introduction

In recent years, infertility has emerged as a significant global concern, affecting approximately 8–12% of couples of reproductive age [1]. Assisted reproductive technology (ART) offers a beacon of hope, with over 10 million babies born worldwide due to its advancements [2]. However, approximately 10% of couples undergoing IVF experience recurrent implantation failure (RIF) [3]. Although a universally accepted definition of RIF does not exist, aspects such as the number of embryo transfers, the quantity of transferred embryos based on differing morphologies, euploidy status, and maternal age are considered. The consensus among most clinicians is that RIF can be characterized as the failure to achieve pregnancy after three fresh or frozen embryo transfers. We adopted the criteria of the Preimplantation Genetic Diagnosis (PGD) Consortium of the European Society of Human Reproduction and Embryology (ESHRE), which defines RIF as more than three failed embryo transfers with high-quality embryos or the failed transfer of 10 or more embryos in multiple cycles [4]. The reasons behind recurrent implantation failure are multifaceted and can be grouped into several categories: embryonic factors, maternal conditions, and the synchronization between the endometrium and the embryo [5]. Among these, endometrial receptivity and thickness play pivotal roles. On one hand, the thickness of the endometrium reflects the structural integrity and functional capacity of the endometrial lining. Notably, patients with thin endometria, constituting 1–2.5% of cases in most ART studies, frequently experience recurrent implantation failure [6], and these patients also have significantly lower rates of ongoing pregnancies and live births. On the other hand, endometrial receptivity is regulated by a complex interplay of molecular and cellular factors, including the interplay between stromal and epithelial cells, and the levels of hormones, cytokines, and growth factors.

Several studies have investigated various aspects of impaired endometrial function underlying RIF, underscoring the importance of the proliferation, differentiation, and interplay between epithelial cells and stromal cells. Wang et al., through single-cell sequencing analysis of post-intercourse endometrial samples and embryos from pregnant mice, found that embryonic implantation released signaling molecules *Pdgfa* and *Efna3/4* to activate differentiation in maternal endometrial epithelial

cells and establish endometrial receptivity [7]. Lai et al. reported a decreased proportion of dominant NK cells expressing high levels of CD49a and EOMES in RIF patients [8]. These NK cells primarily function to promote fetal growth in early pregnancy by enhancing cell adhesion and tissue remodeling in stromal and epithelial cells through the TNFSF14/TNFRSF14 and MMP9 signaling pathways, and assisting angiogenesis to facilitate trophoblast invasion. Additionally, SFRP4+ stromal cells were noted as key regulators influencing the proliferation of epithelial cells in women with normal fertility [9]. Proliferating stromal (pStromal) cells, which contribute to the growth of stromal cells, were found to have impaired cell cycle signaling pathways in TE-RIF patients [10]. However, the impact of damaged cell signaling pathways in pStromal cells on the function of subsequent stromal cells and endometrial receptivity remains unclear. The intricate communication between stromal cells and epithelial cells is still largely unexplored.

In this study, we aim to study the different etiologies behind impaired endometrial thickness and endometrial receptivity by comparing the transcriptome of endometrium derived from RIF patients with thin endometrium (≤ 6 mm, TE-RIF), normal endometrium (≥ 8 mm, NE-RIF) and fertile individuals (control) group. The insights gained from this study promise to make individualized clinical strategies and therapeutic interventions.

Methods

Sample collection

Zhejiang Provincial People's Hospital approved the use of human tissue for this study (2019QT003). We adopted the criteria for RIF set by the Preimplantation Genetic Diagnosis (PGD) Consortium of the European Society of Human Reproduction and Embryology (ESHRE), which defines RIF as more than three failed embryo transfers with high-quality embryos, or the failed transfer of 10 or more embryos in multiple cycles [4]. TE-RIF (thin endometrium with recurrent implantation failure) patients had a maximum endometrial thickness of ≤ 6 mm throughout the menstrual cycle, while NE-RIF (normal-thickness endometrium with unexplained recurrent implantation failure) participants maintained a normal endometrial thickness of ≥ 8 mm (Supplementary Tables 1–2). Volunteers in the control group had at least one child born naturally and displayed an endometrial

thickness exceeding 8 mm, without a history of infertility or abortion. We enrolled three participants in the TE-RIF group, two in the NE-RIF group, and three in the control group. Among the eight participants, one from the control group and one from the TE-RIF group were from our previous study [11]. Inclusion criteria included age under 35, a regular menstrual cycle lasting 26–30 days, normal ovulation, non-smoking habits, and the absence of abnormalities in metabolism, blood coagulation, immune system, and reproductive system, such as polycystic ovary syndrome, polyps, adenomyosis, endometritis, and tumors. Exclusion criteria included the presence of an intrauterine device or having received any endometrial therapy within the past month.

Biopsies of the endometrium were obtained from the anterior or posterior wall during the late proliferative phase (1–2 days before ovulation) and the mid-secretory phase (6–7 days after ovulation) in a natural cycle. Dating was performed with ultrasound scans and hormone levels (Supplementary Table 1), and histological dating of the endometrial samples was consistent with the menstrual cycle phases (Fig. 1B).

Sample preparation

Each endometrial sample was approximately 100 mm³ in size. After collection, the samples were promptly immersed in 0.9% cold sodium chloride and transported on ice to ensure cell viability. Following this, the

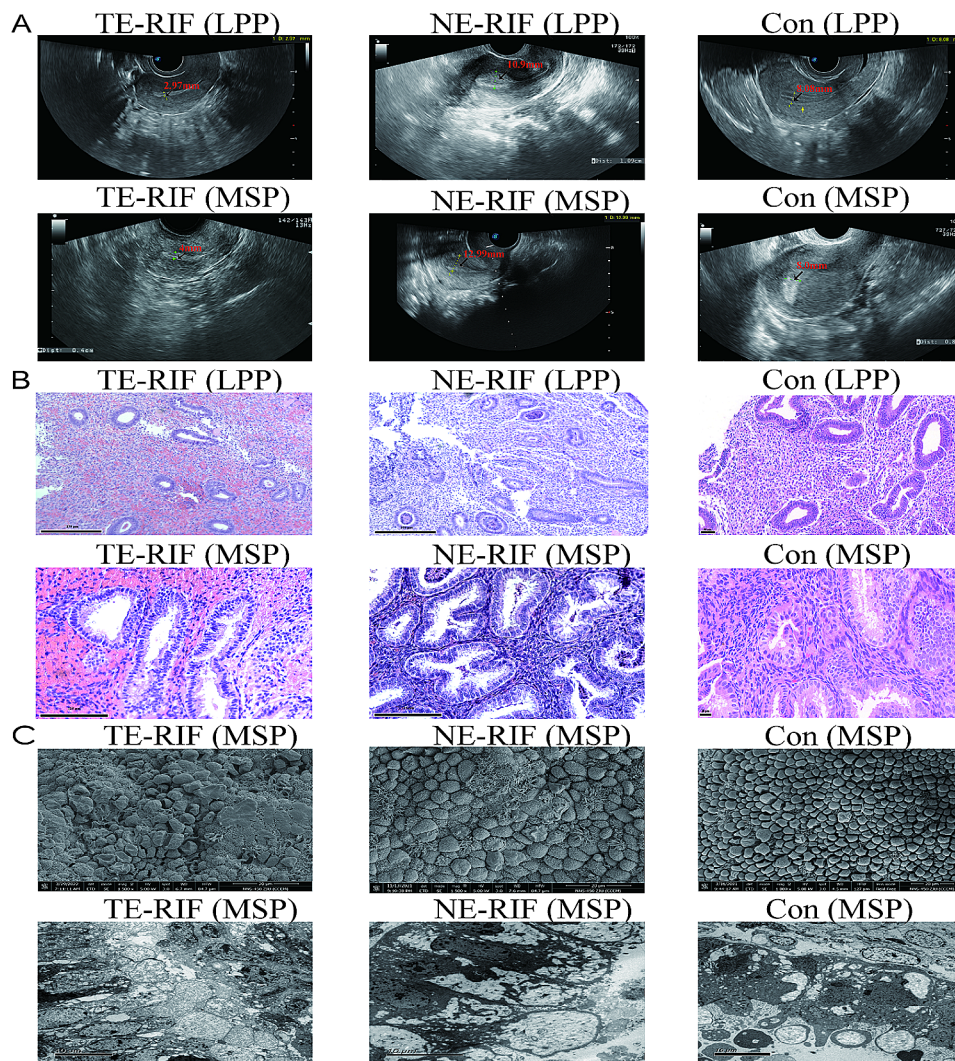


Fig. 1 Comparison of clinical examination results among three groups. (A) Representative ultrasound images of endometrial thickness for the TE-RIF, NE-RIF, and control groups in the late proliferation phase and middle secretory phase. (B) Representative hematoxylin and eosin staining of TE-RIF, NE-RIF, and control samples at the late proliferative phase and mid-secretory phase. (C) Comparison of the quality and number of secretory vesicles for the TE-RIF, NE-RIF, and control samples, detected by scanning electron microscopy; comparison of the number of secretory cells for the TE and control samples, detected by transmission electron microscopy. TE-RIF: recurrent implantation failure patients with thin endometrium, NE-RIF: recurrent implantation failure patients with normal endometrium thickness, control: fertile volunteers

endometrial tissue underwent a thorough rinse with phosphate-buffered saline (PBS, BIOIND, USA) and Dulbecco's Modified Eagle Medium (DMEM, Gibco, USA) before being finely dissected into smaller fragments. Subsequently, the dissected tissue was transferred into a digestive solution (Sigma, USA) containing 1.5 mg/ml type I collagenase. The mixture was gently shaken at 4 °C and incubated for 7–8 h to obtain cell suspensions. The cell suspension was filtered through a 40 µm nylon strainer (BD Falcon, USA) and centrifuged at 1500 rpm for 6 min. The supernatant was discarded. Next, a digestion solution containing 0.25% trypsin-EDTA (Gibco, USA) and 2.3 mg/ml DNase I (Roche, Switzerland) was introduced. Sequential incubation steps were carried out at 37 °C for 5 min each. An equal volume of DMEM/F12-10% FBS (BIOIND, USA) was then added before another round of centrifugation. Red blood cells were lysed using an RBC lysis buffer (Beyotime, China) at room temperature, followed by another centrifugation. The resulting pellet was retained. Trypan blue (Sigma, USA) staining was used to determine cell viability. Finally, the cells were suspended in PBS at a density of 1×10^5 cells/100 µl for single-cell sequencing.

Single-cell RNA-seq data processing

RNA sequencing was conducted using 10x Genomics technology, and the Cell Ranger software (v.6.1.2) was employed to decode gene expression and align reads to the reference genome (GRCh38). For each individual sample, matrices for gene and cell counts were created (Supplementary Table 3). Using “Cellranger aggr” to aggregate multiple samples, the R package Seurat (v.4.1.1) was then used for downstream analysis (Resolution: 0.8, Dims used for cell clustering: 20). Cells expressing more than 500 genes and with less than 25% mitochondrial gene expression were included [12, 13]. The filtered gene expression matrix was normalized using the NormalizeData function, which employs the global-scaling normalization method “LogNormalize”. The normalized gene expression matrix generated after preprocessing was used to cluster cells and visualized by dimension reduction. In brief, 2000 highly variable genes were selected, and then principal component analysis (PCA) based on the z-transformed expression values of the identified highly variable genes was performed. The top 20 were used for clustering by uniform manifold approximation and projection (UMAP) for dimension reduction with a resolution of 0.8. Cluster identities were assigned based on the differentially expressed genes (DEGs) for each cluster, as determined by the FindMarkers function (with parameters: $p\text{-value} \leq 0.01$ and $\text{Log}_2\text{FC} \geq 0.26$), and gene expression of known marker genes.

Enrichment analysis

The combined approach of KEGG and GO enrichment analysis served to illuminate the intricate interplay of genes within broader biological pathways and functional categories [13, 14]. The differentially expressed genes (DEGs) were used for enrichment analysis by the OmicStudio platform (<https://www.omicstudio.cn/home?slide=2>).

Construction of single-cell trajectories

The Python package scVelo (Python version 0.2.5.1) was employed to construct single-cell trajectories in pseudotime order by calculating the RNA velocity (<https://scvelo.readthedocs.io/en/stable/>). This analysis was pivotal in uncovering the directional trends in gene expression changes, enabling us to unravel the complex relationships between stromal cells and epithelial cells during their differentiation processes.

Cell communication

To figure out the communication between different cell types, CellPhoneDB (www.cellphonedb.org, v3) was used to analyze the interaction between proteins secreted by epithelial and stromal cells in different groups [15]. Normalized counts and cell type annotation information were inputted and combined. The percentage of cells expressing the gene and the mean value of gene expression were calculated. A ligand-receptor pair was included in the analysis when the percentage of cells expressing both receptor and ligand genes exceeded 10%. All cells were randomly arranged to form a new cell population (the default number of random arrangements was 1000 times). The average expression level of the ligand in the cell population after random arrangement and the average expression level of the receptor in the cell type with which it interacted were calculated, and then an average mean was calculated. This process was repeated many times to obtain a mean null distribution. After the null distribution was generated, the actual mean of the ligand-receptor pair between the two cell types was calculated according to the original cell clustering, and the possible significance p-value of the ligand-receptor pair in the two cell types was inferred from the proportion of the calculated mean that was equal to or higher than the actual mean. Finally, highly specific interactions between cell types were ranked according to the number of significant ligand-receptor pairs enriched in both cell types to allow manual screening of biologically relevant interaction relationships.

Hematoxylin and eosin staining

Tissue sections (3 µm) from formalin-fixed, paraffin-embedded human endometrium underwent HE staining. The process involved dewaxing, hydration, staining with

hematoxylin and eosin, dehydration, and sealing. Imaging was performed using a Nikon ECLIPSE E100 microscope and Nikon DS-U3 imaging software.

Scanning and transmission electron microscopy

Scanning Electron Microscope (SEM): Tissues fixed in 2.5% glutaraldehyde were first rinsed with PBS, then fixed in 1% osmic acid for 1.5 h and again rinsed in PBS. This was followed by a series of alcohol dehydrations (50%, 70%, 90%, 100%). Samples were examined using the SEM Nova Nano450 (Thermo Fisher FEI, USA).

Transmission Electron Microscope (TEM): After fixation in 2.5% glutaraldehyde and rinsing in PBS, tissues were fixed in 1% osmic acid for 1.5 h, washed in PBS, and stained with 2% uranyl acetate (HEAD, China). A sequential alcohol dehydration was employed. The tissues were then infiltrated using a mixture of embedding agent and pure propionic acid (Guidechem, China) in ratios of 1:1 and 3:1, embedded in resin (ChemNet, China), polymerized, and fixed. The examination was conducted using an electron microscope (Thermo Fisher Scientific, MA, USA). For methodology details, please see our prior research [11].

Immunohistochemistry (IHC)

Immunohistochemical staining was conducted on 3 μ m formalin-fixed paraffin-embedded human endometrium. The protocol included dewaxing, rehydration, antigen retrieval, peroxidase blocking, primary and secondary antibody incubation, DAB staining, counterstaining with Harris hematoxylin, and subsequent dehydration and sealing, as described in our previous research [11]. Microscopic examination was performed using a CIC XSP-C204 microscope. Primary antibodies used were as follows: GZMK, COL1A1, VWF, FGFBP2, GNLY, CD3D, FOXJ1, PCDH9, DCN, PECAM1, GZMB, ALDOC, KLRC1, FAM183A, HLA-DRA, and STMN1 (all sourced from Servicebio, Bioss, Proteintech, Abcam, and Abclonal in China, and ATLAS antibodies in Sweden).

Statistical analysis

Data were presented as means \pm SD. Gene expressions in three groups were compared and analyzed by the Wilcoxon rank-sum test or ANOVA test in GraphPad Prism9 (GraphPad Software, La Jolla, CA, USA), and mentioned in the legend. A p -value < 0.01 was considered statistically significant in the comparison of gene expression among the TE-RIF samples, NE-RIF samples, and control samples.

Results

Morphology of the endometrium

Ultrasound was employed to assess the endometrial thickness (Fig. 1A). In the late proliferative phase (LPP),

HE-stained sections from the control group showed round and closely arranged stromal cells, proliferated and spirally coiled small arteries within the stroma, an increased number of glands, and enlarged and slightly curved glandular cavities (Fig. 1B). Conversely, the TE-RIF group exhibited relatively loose stromal cells, fewer spiral curly arterioles, a reduced glandular count, and flatter luminal structures (Fig. 1B). The NE-RIF group demonstrated better characteristics compared to the TE-RIF group (Fig. 1B).

After transitioning to the mid-secretory phase (MSP), the endometrial glands in the TE-RIF group did not exhibit the expected curvature and hypertrophy characteristics seen in the control group. Similarly, stromal cells in the TE-RIF group did not display the loose or edematous characteristics typical of this phase, while the endometrial epithelial glands in the NE-RIF group showed slight curvature without significant expansion of glandular cavities or secretion (Fig. 1B) [16].

In addition, SEM results demonstrated that both TE-RIF and NE-RIF patients in the MSP phase had fewer fully developed endometrial pinopodes, which appeared shrunken and immature, mostly suggesting regressing pinopodes (Fig. 1C). In contrast, the control group displayed developing and fully developed pinopodes with abundant microvilli (Fig. 1C). In terms of supranuclear secretion observed by TEM, the control group exhibited relatively rich secretory content, while the TE-RIF group displayed predominantly subnuclear secretion (Fig. 1C). These findings suggested that the endometrial receptivity in TE-RIF and NE-RIF patients was impaired [17–19].

Single-cell atlas of the endometrium

To further explore the mechanism of impaired endometrial receptivity, single-cell RNA sequencing was performed on endometrium samples from eight participants in both the late proliferative and mid-secretory phases, resulting in a total of 16 samples. After filtering, an unbiased clustering approach identified 102,920 cells, which were subsequently categorized into ten distinct cell types across 21 clusters (Fig. 2A–C). The predominant cell type, marked by *COL1A1* and *DCN*, was stromal cells with a subset identified as proliferating stromal cells (pStromal) characterized by the expression of *MKI67*, *PCNA*, and *STMN1* [9, 10, 20, 21]. Epithelial cells were identified by high expression levels of *KRT18* and *EPCAM* [9], while ciliated epithelial cells were marked by *FAM183A* and *FOXJ1* [22]. NK cells were identified by *GNLY* and *KLRC1* [10], endothelial cells by *PECAM1* and *VWF* [8, 9], T cells by *CD3D* and *GZMK* [23, 24], B cells by *CD74* and *HLA-DRA* [25, 26], NK T cells by *GZMB* and *FGFBP2* [27], and pNK cells by *PCDH9* and *ALDOC* [10] (Fig. 2D).

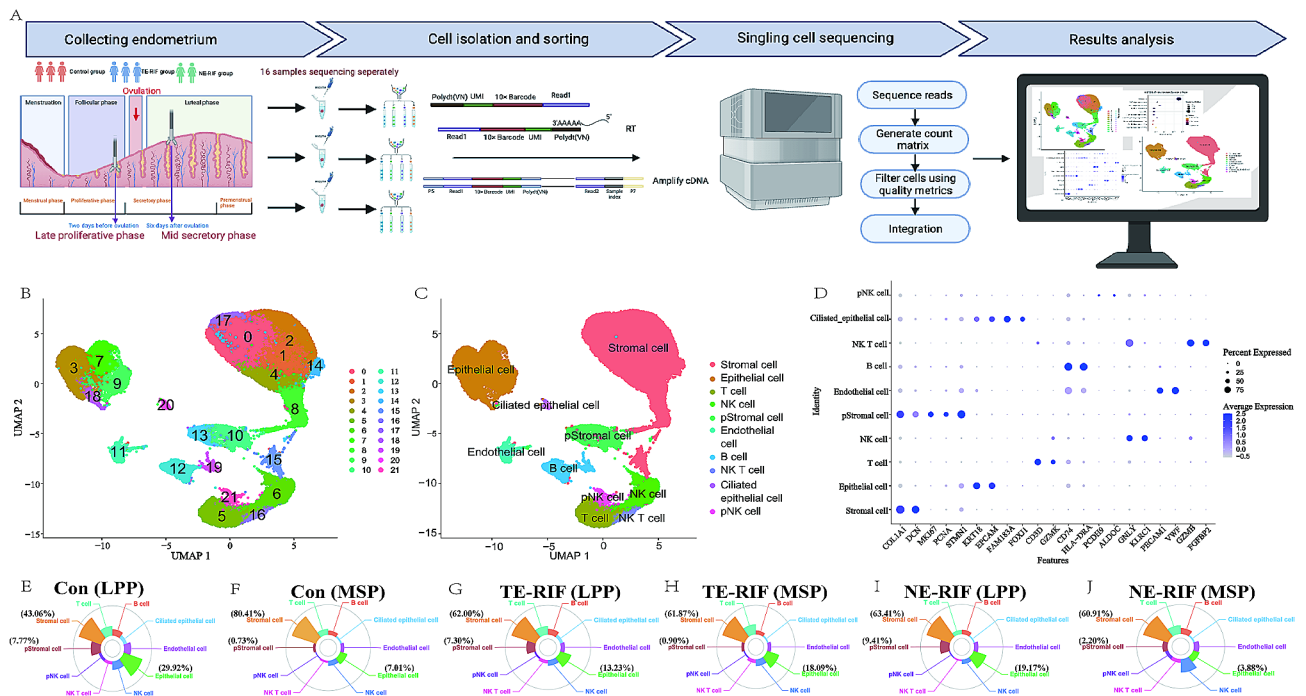


Fig. 2 Comparison of the proportion of different cell types. **(A)** Summary of sample collection, single-cell sequencing, and analysis workflow. **(B)** UMAP (uniform manifold approximation and projection) plot consisting of 21 clusters colored by differential clusters. **(C)** UMAP plot of 102,920 single cells colored by major cell lineages, with each dot representing an individual cell. **(D)** Mean expression of classical marker genes for each cell type in the endometrial samples. **(E–J)** Nightingale rose diagrams showing the distribution of cell fractions of each cell type across the TE-RIF, NE-RIF, and control groups in the late proliferative phase and the mid-secretory phase. TE-RIF ($n=3$): recurrent implantation failure patients with thin endometrium, NE-RIF ($n=2$): recurrent implantation failure patients with normal endometrium thickness, control ($n=3$): fertile volunteers

Delving into the shifting proportions of distinct cell types, we observed intriguing patterns. In the control group, stromal cells constituted merely 43.06% in LPP, which surged to 80.41% during MSP (Fig. 2E–F, Supplementary Table 3). Strikingly, unlike the control group, neither the TE-RIF group (from 62.00 to 61.87%) nor the NE-RIF group (from 63.41 to 60.91%) exhibited a twofold surge in stromal cell proportions (Fig. 2G–J, Supplementary Table 4).

In terms of the percentage of epithelial cells, the control group experienced a marked 12% decline in MSP compared to the LPP (from 29.92 to 17.01%), and the NE-RIF group exhibited a similar pattern, while the TE-RIF group demonstrated a contrasting trend (from 13.23 to 18.09%) (Fig. 2G–J, Supplementary Table 4). Considering that epithelial and stromal cells are key players in the endometrium, these imbalances in their proportions during the menstrual cycle imply endometrial growth asynchrony.

Remarkably, a parallel shift in the proportion of pStromal cells was observed in both the control and TE-RIF groups. Intriguingly, the NE-RIF group displayed a higher proportion of pStromal cells compared to the control group in both phases (Fig. 2I–J, Supplementary Table 4).

Dysregulation of cell cycle in stromal cells

In our quest to uncover the factors contributing to the resistance of thin endometrium to thickening, we embarked on an exploration of gene expressions in pStromal cells. Among the top 10 markers in clusters 10 and 13, *MKI67* and *STMN1* emerged, corroborated by a previous study as indicative of pStromal cells [10]. Remarkably, *MKI67* was identified as a marker gene for pStromal cells, associated with the G2 phase and mitosis [28–30] (Fig. 3A–B). GO analysis confirmed enrichment of biological processes pertinent to pStromal cells, including protein binding, cell cycles, and cell division (Fig. 3C). To ascertain potential functional impairments in pStromal cells, we conducted a gene expression comparison between the control and TE-RIF groups in LPP. The resulting volcano plot showcased 206 genes expressed at significantly elevated levels and 208 genes at significantly diminished levels. Notably, genes such as *CREB5*, *FOS*, *JUNB*, and *JUN*, known regulators of the cell cycle, exhibited upregulation (Fig. 3I). Their overexpression could disrupt cell cycle regulation, potentially leading to premature apoptosis [31–33]. RNA velocity analysis illuminated the differentiation trajectory of pStromal cells into stromal cells in LPP, implying the potential impact of abnormal pStromal cell expression on stromal cells (Fig. 3E–G). This trend resonated in

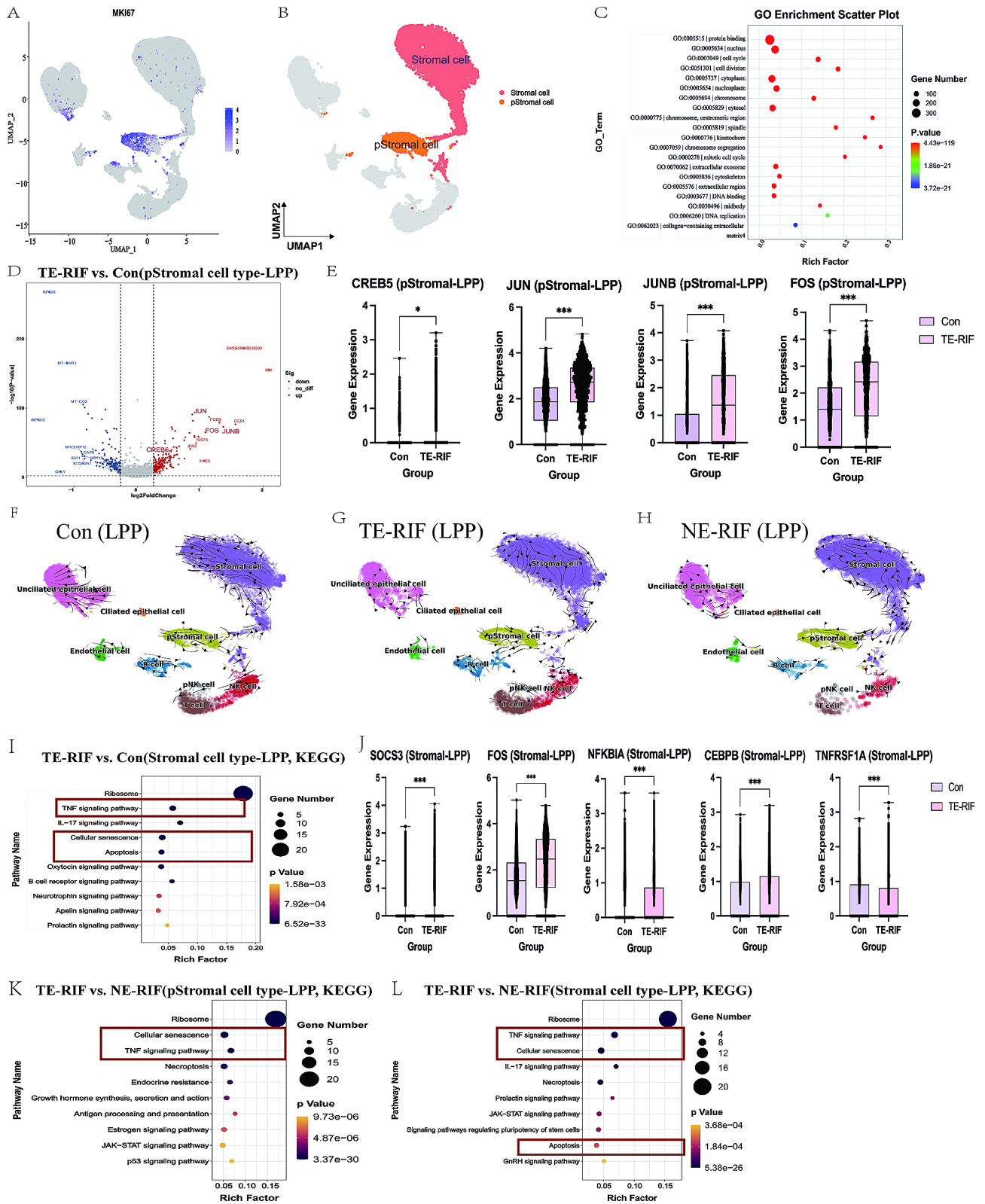


Fig. 3 (See legend on next page.)

(See figure on previous page.)

Fig. 3 Distribution of key transcription factors in stromal cells between the TE-RIF and control samples in late proliferative phase. **(A)** Cell distribution and expression of *MKI67* for pStromal cells from all samples. **(B)** UMAP (uniform manifold approximation and projection) plot highlighting the distribution of pStromal and stromal cells. **(C)** GO (Gene Ontology) enrichment analysis for pStromal cells ($p < 0.01$, $\log FC < 0.26$ & $\log FC > -0.26$). **(D)** Volcano plot depicting gene expression differences between pStromal cells of the TE-RIF group and the control group in LPP ($p < 0.01$, $\log FC < 0.26$ & $\log FC > -0.26$). **(E)** Box plot showing the expression of key genes in cell cycle regulation (purple: control group, pink: TE-RIF group). **(F-H)** RNA velocity of the TE-RIF, NE-RIF, and control groups in the late proliferative phase. **(I)** KEGG (Kyoto Encyclopedia of Genes and Genomes) enrichment analysis of upregulated differentially expressed genes in stromal cells of the TE-RIF group compared to the control group in LPP ($p < 0.01$, $\log FC < 0.26$ & $\log FC > -0.26$). **(J)** Box plot showing the expression of key genes in the TNF signaling pathway (purple: control group, pink: TE-RIF group). **(K, L)** KEGG enrichment analysis of upregulated differentially expressed genes in pStromal cells **(K)** and stromal cells **(L)** of the TE-RIF group compared to the NE-RIF group in the late proliferation phase ($p < 0.01$, $\log FC < 0.26$ & $\log FC > -0.26$). Wilcoxon test: * $p < 0.033$, *** $p < 0.001$. TE-RIF: recurrent implantation failure patients with thin endometrium, NE-RIF: recurrent implantation failure patients with normal endometrium thickness, control: fertile volunteers

the KEGG analysis, where stromal cells of the TE-RIF group in LPP exhibited enrichment in apoptosis and cellular senescence signaling pathways (Fig. 3H). The TNF (tumor necrosis factor) signaling pathway, crucial for cell cycle regulation, emerged as the second significantly enriched pathway. Key genes such as *TNFRSF1A*, *CEBPB*, *NFKBIA*, *SOCS3*, and *FOS* showed higher expression in stromal cells from the TE-RIF group compared to those in the control group in LPP (Fig. 3J). TNF- α signaling triggers inflammation and apoptosis, and the emergence of suppressor of cytokine signaling 3 (*SOCS3*) curbs ongoing NF- κ B activation, fostering apoptosis [34]. In conclusion, we surmised that one contributing factor to the resistance of thin endometrium to thickening in TE-RIF patients might be the accelerated apoptosis of stromal cells. Aberrant TNF signaling pathways, potentially linked to abnormal activation, might underlie this phenomenon.

Recent reports have highlighted the profound impact of cellular senescence on endometrial receptivity [35]. Correspondingly, marker genes such as *IGFBP2*, *PGR*, *HAND2*, *FOXO1*, *HOXA10*, and *HOXA11* exhibited reduced expression levels in stromal cells of the TE-RIF group during the MSP (Fig. 4A) [36]. KEGG analysis of stromal cells from both the control and TE-RIF endometrium in MSP continued to reveal enrichment in apoptosis and cellular senescence pathways (Fig. 4B). This observation led us to infer that accelerated senescence of pStromal cells could potentially affect subsequent function of stromal cells. Notably, the MAPK (mitogen-activated protein kinases) signaling pathway emerged as a pivotal mediator within this context (Fig. 4B). Taking a closer look at the MAPK signaling pathway, we identified highly expressed genes including *TNFRSF1A*, *RRAS*, *MYC*, *HSPA1A*, *JUND*, and *FOS* (Fig. 4C-D). This pathway not only regulates stromal cell progesterone sensitivity adjustments but also wields significant influence over cellular senescence and inflammation outcomes [37–39]. The delicate balance in MAPK signaling ensures proper stromal cell function, while excessive activation might culminate in cellular senescence and inflammatory cascades. This interplay between cellular senescence, MAPK signaling, and stromal cell dynamics underscores the

intricacies governing endometrial receptivity. It highlights how abnormalities at the pStromal cell level could cascade into significant disruptions in subsequent stages of stromal cell maturation, ultimately impacting endometrial receptivity.

Compared to the NE-RIF group, KEGG analysis of differentially upregulated genes in pStromal cells of the TE-RIF group showed that cell senescence and the TNF signaling pathway were still enriched pathways (Fig. 3K). The same phenomenon was observed when gene expressions in stromal cells were compared between the two groups, further indicating dysregulation in the stromal cell cycle in TE-RIF patients (Figs. 3L and 4E).

Insensitive epithelial cells and decreased adhesion

The gradual proliferation of epithelial cells and their altered adhesion had significant implications, particularly in light of the direct interaction between embryonic trophoblasts and the luminal epithelium, which is crucial for uterine receptivity [40]. Notably, our KEGG analysis revealed downregulation of gene expression in the estrogen signaling pathway in epithelial cells of the TE-RIF group compared to the control group in LPP (Fig. 5A). This pathway plays a key role in promoting cellular growth. Thus, we further investigated the expression of *ESR1*, a gene responsible for synthesizing a critical regulatory hormone that governs endometrial growth in LPP [41]. Strikingly, *ESR1* expression was found to be lower in the TE-RIF group in both LPP and MSP (Fig. 5B-C). This indicated an insufficient estrogen response to support epithelial cell growth in LPP, thereby limiting their proliferation. Moreover, considering the role of progestogens in driving epithelial cells into a receptive state, the lowered expression of *PGR* in epithelial cells during the MSP of the TE-RIF group substantiated their unpreparedness for embryo implantation [42] (Fig. 5D).

Further scrutinizing the epithelial cells of the TE-RIF group in MSP, we noted the downregulation of genes associated with the ECM-receptor signaling pathway, offering another crucial insight into embryo implantation failure (Fig. 5F). Within it, extracellular matrix (ECM)-related genes, including *COL1A1*, *COL1A2*, *COL6A1*, *COL4A1*, *COL4A2*, *SPPI*, *LAMB1*, and *FREM2* alongside

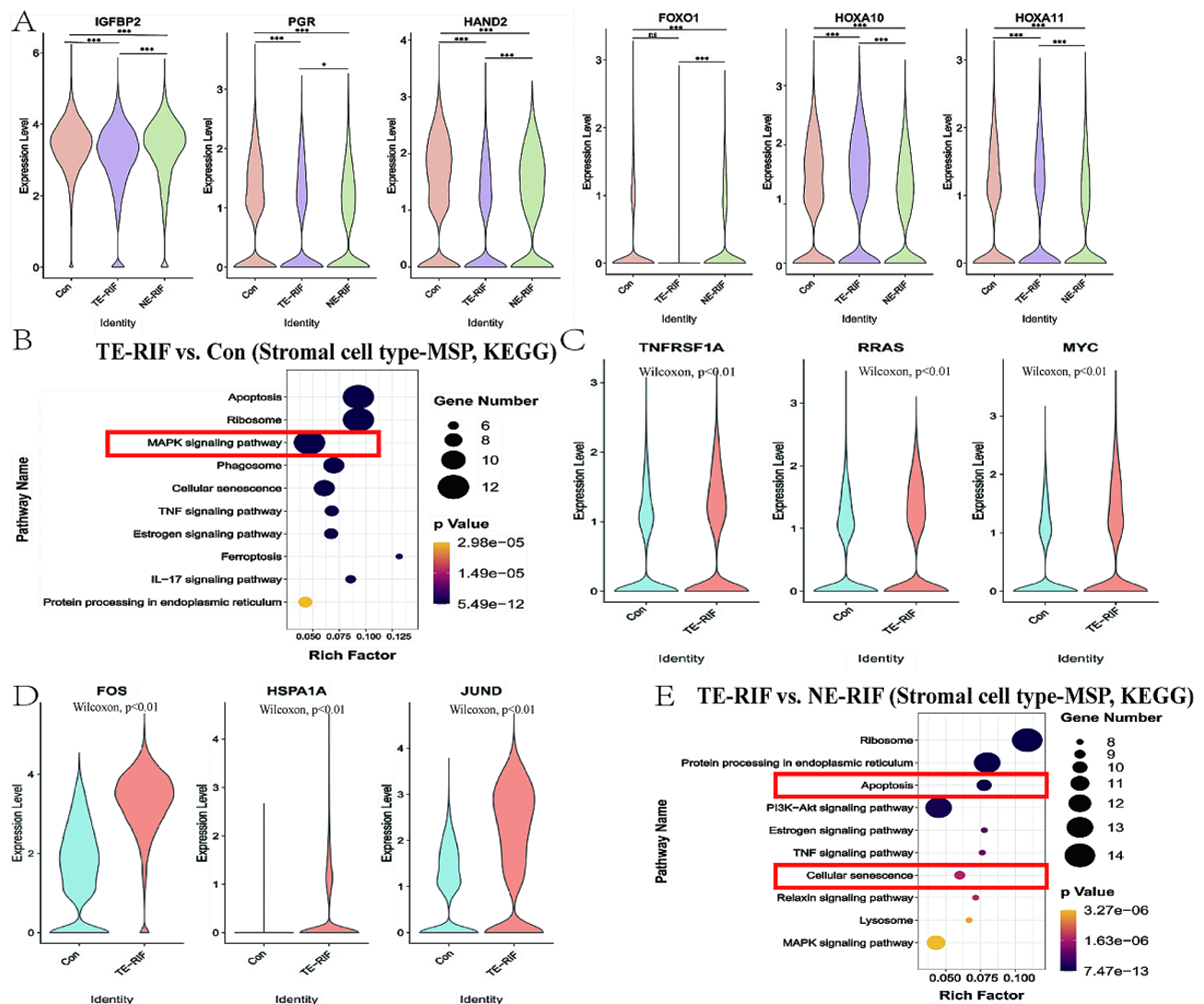


Fig. 4 Distribution of key transcription factors in stromal cells between the TE-RIF and control groups in mid-secretory phase. **(A)** Violin plots showing differences in the expression of marker genes related to endometrial decidualization among the TE-RIF, NE-RIF, and control groups in stromal cells during the mid-secretory phase. Wilcoxon test: * $p < 0.033$, *** $p < 0.001$. Orange: control, purple: TE-RIF, green: NE-RIF. **(B)** KEGG (Kyoto Encyclopedia of Genes and Genomes) enrichment analysis of upregulated differentially expressed genes in stromal cells between the TE-RIF and control groups in the mid-secretory phase ($p < 0.01$, $\log FC < 0.26$ & $\log FC > -0.26$). **(C-D)** Violin plots showing the expression of key genes in the MAPK signaling pathway of stromal cells in the mid-secretory phase. **(E)** KEGG enrichment analysis of the upregulated differentially expressed genes in stromal cells of the TE-RIF group compared to the NE-RIF group in the mid-secretory phase ($p < 0.01$, $\log FC < 0.26$ & $\log FC > -0.26$). TE-RIF: recurrent implantation failure patients with thin endometrium, NE-RIF: recurrent implantation failure patients with normal endometrium thickness, control: fertile volunteers

their receptors (*ITGA6*, *ITGB8*, and *ITGB1*), manifested low expression in the TE-RIF group (Fig. 5E, G-H). The intricate process of trophoblastic invasion during the implantation window necessitates robust epithelial cell adhesion, essential for embryo recognition, attachment, and tissue repair. The ECM plays an important role in maintaining endometrial structure, facilitating differentiation, and ensuring embryo nutrition. Their suppressed expression implied that the endometrium, during the implantation window, struggled to establish normal communication with the embryo and create a conducive implantation environment.

When we performed KEGG analysis of the differentially expressed genes in epithelial cells between the TE-RIF group and the NE-RIF group, it was found that the downregulated genes in the TE-RIF group were enriched in the estrogen signaling pathway during LPP. This suggested a significant impairment in the response of epithelial cells to estrogen stimulation during this phase, potentially affecting their subsequent sensitivity to progesterone [43]. Interestingly, compared to the TE-RIF group, we observed downregulation of the ECM-receptor signaling pathway in the NE-RIF group during MSP (Fig. 5J). Simultaneously, we detected abnormal

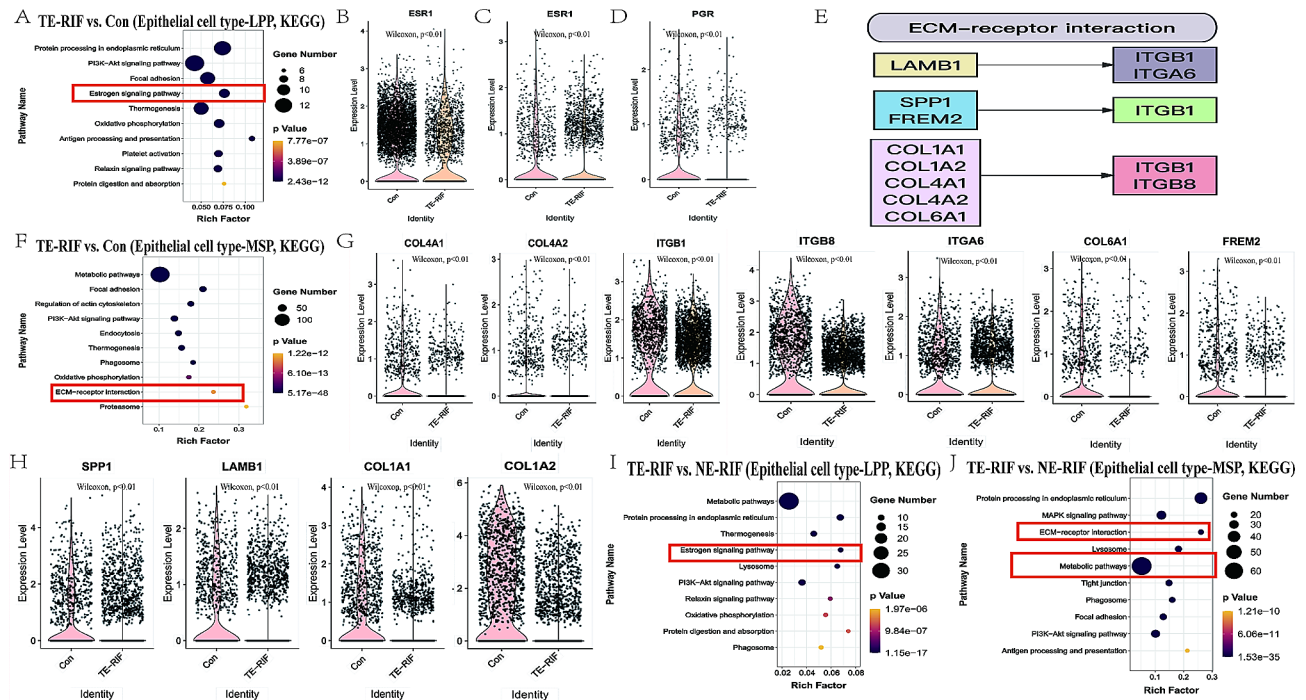


Fig. 5 Distribution of key transcription factors in epithelial cells between the TE-RIF and control groups. **(A)** KEGG (Kyoto Encyclopedia of Genes and Genomes) enrichment analysis for downregulated differentially expressed genes in epithelial cells between the TE-RIF and control groups in the late proliferative phase ($p < 0.01$, $\log FC < 0.26$ & $\log FC > -0.26$). **(B, C)** Expression of *ESR1* in epithelial cells in the late proliferative phase **(B)** and mid-secretory phase **(C)**. Peach orange: TE-RIF, wax flower: control. **(D)** Expression of *PGR* in epithelial cells during the mid-secretory phase. **(E)** Interactions between various collagens and integrins. **(F)** KEGG enrichment analysis of downregulated differentially expressed genes in epithelial cells between the TE-RIF and control groups in the mid-secretory phase. **(G-H)** Expression of key genes in the ECM-receptor interaction signaling pathway in epithelial cells during the mid-secretory phase. **(I, J)** KEGG enrichment analysis of downregulated **(I)** and upregulated **(J)** differentially expressed genes in epithelial cells of the TE-RIF group compared to the NE-RIF group in the late proliferative phase ($p < 0.01$, $\log FC < 0.26$ & $\log FC > -0.26$). TE-RIF: recurrent implantation failure patients with thin endometrium, NE-RIF: recurrent implantation failure patients with normal endometrium thickness, control: fertile volunteers

metabolic pathways in NE-RIF patients, which could lead to dysfunction of protein and lipid synthesis in epithelial cells (Fig. 5)). This dysfunction may explain the impaired synthesis of extracellular matrix collagen, which is critical for facilitating embryo implantation [44].

Successful implantation requires cooperative interaction between epithelial and stromal cells, and there are differing opinions on whether epithelial-mesenchymal transition (EMT) actually occurred [35, 45]. RNA velocity was employed to study cell development, and our data did not show evidence of EMT (Fig. 3F-H). This suggested that in normal endometrium, epithelial cells do not undergo transformation from stromal cells, and due to challenges in obtaining full-thickness endometrium, the specific origin of epithelial stem cells remains uncertain. While the existence of EMT or MET in the endometrium has not been proven, the communication between stromal cells and epithelial cells remains a crucial area for investigation.

Cell communication

Optimal uterine receptivity and successful embryo implantation require effective communication between

the epithelial and stromal cells [40, 46]. CellPhoneDB analysis indicated higher cell communication activity in the TE-RIF group compared to the control group in LPP (Fig. 6A-B). However, by observing the top 20 ligand-receptor pairs, *WNT5A-SFRP4* was found to be active in epithelial-stromal cell communication in the control group and not active in the TE-RIF group (Fig. 6C, Supplementary Tables 5–6). Wu's article also noted that stromal cells expressing *SFRP4* had a significant proportion in the proliferative phase, and when these cells were co-cultured with epithelial cells, the cell growth rate was significantly increased [9]. *WNT5A* encodes a member of the WNT family that is related to the growth of epithelial glands, and the expression levels of *WNT5A* and *SFRP4* change with the menstrual cycle [47, 48]. This suggests that WNT-SFRP4 might be a key target for the impaired proliferation of epithelial cells due to abnormal communication between stromal and epithelial cells in thin endometrium.

In MSP, we observed strong intercellular communication in the control group, where interactions between endothelial cells and B cells were extremely active (Fig. 6D-E). In contrast, compared to the control group,

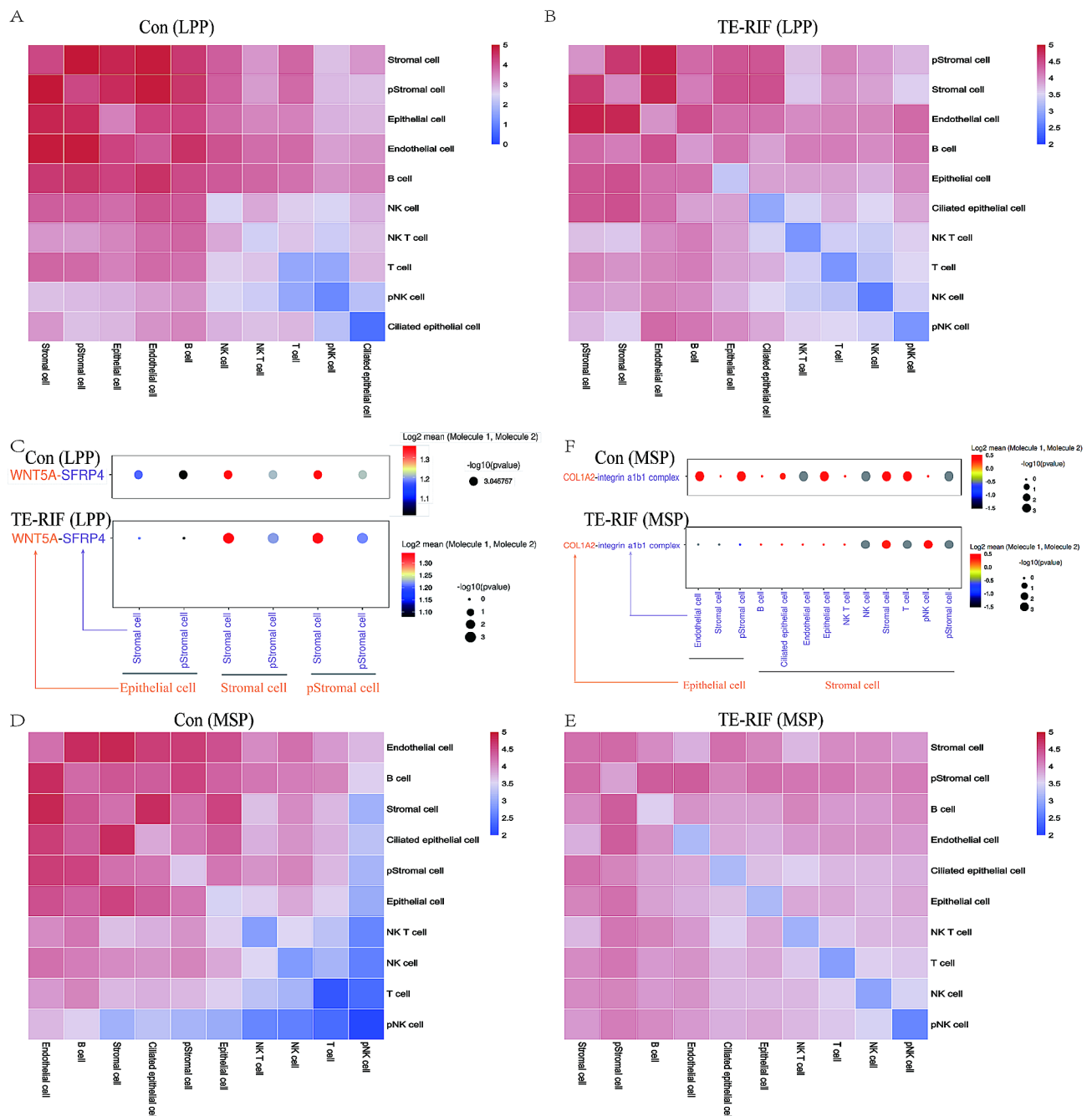


Fig. 6 Cell communication in the TE-RIF and control groups. **(A, B)** Heatmaps showing cell-cell communication in the control group **(A)** and the TE-RIF group **(B)** during the late proliferative phase. **(C)** Dot plot showing the extracted ligand-receptor pair of WNT5A-SFRP4 in the control group (top) and in the TE-RIF group (bottom) during the late proliferative phase. **(D, E)** Heatmaps showing cell-cell communication in the control group **(D)** and the TE-RIF group **(E)** during the mid-secretory phase. **(F)** Dot plot showing the extracted ligand-receptor pair of COL1A2-integrin $\alpha 1\beta 1$ in the control group (top) and the TE-RIF group (bottom) during the mid-secretory phase. TE-RIF: recurrent implantation failure patients with thin endometrium, NE-RIF: recurrent implantation failure patients with normal endometrium thickness, control: fertile volunteers

we found that the COL1A2-integrin $\alpha 1\beta 1$ ligand-receptor pair was not as active between stromal cells and epithelial cells in the TE-RIF group (Fig. 6F, Supplementary Tables 7–8). This might indicate that the secretion of collagen and integrin was not sufficient in thin endometrium,

which is related to the communication between stromal cells and epithelial cells.

Metabolic disruptions in the NE-RIF group

The KEGG analysis unveiled significant upregulation of metabolic pathways in both pStromal and stromal cells

in the NE-RIF group compared to the control group (Fig. 7A-C). This heightened metabolic activity suggested a metabolic disorder in NE-RIF patients. Notably, stromal cells exhibited abnormal collagen deposition and focal adhesion, with overexpression of genes related to types I and VI collagen and integrins (Fig. 7D-F). Focal adhesion plays an important role in the remodeling of the extracellular matrix and cell motility. The aberrant transcriptional activation of collagen genes caused defects in decidualization [49, 50]. Furthermore, in epithelial cells, we observed increased activity in carbohydrate metabolism pathways, such as fructose and mannose metabolism in the late proliferative phase and carbon metabolism in the mid-secretory phase (Fig. 7G-H). This might explain the improper carbohydrate metabolism, potentially detrimental to embryo implantation [51, 52].

Discussion

In our study, we performed a comprehensive analysis of scRNA-seq data of the endometrium from TE-RIF patients, NE-RIF patients, and volunteers with normal fertility. Our investigation into stromal cell differentiation and gene expression revealed dynamic changes and identified the TNF and MAPK signaling pathways as being associated with defective endometrial receptivity. Additionally, we constructed a cell-cell interaction network, highlighting the importance of communication between stromal and epithelial cells for endometrial growth and receptivity. Furthermore, we discovered that a metabolic disorder was the primary challenge for NE-RIF patients. These findings provide valuable information for optimizing therapy for TE-RIF and NE-RIF patients.

In this study, we gained a more comprehensive understanding of the cell types in different phases of the endometrium. The percentage of pStromal cells was found to be overall consistent among the three groups, but the

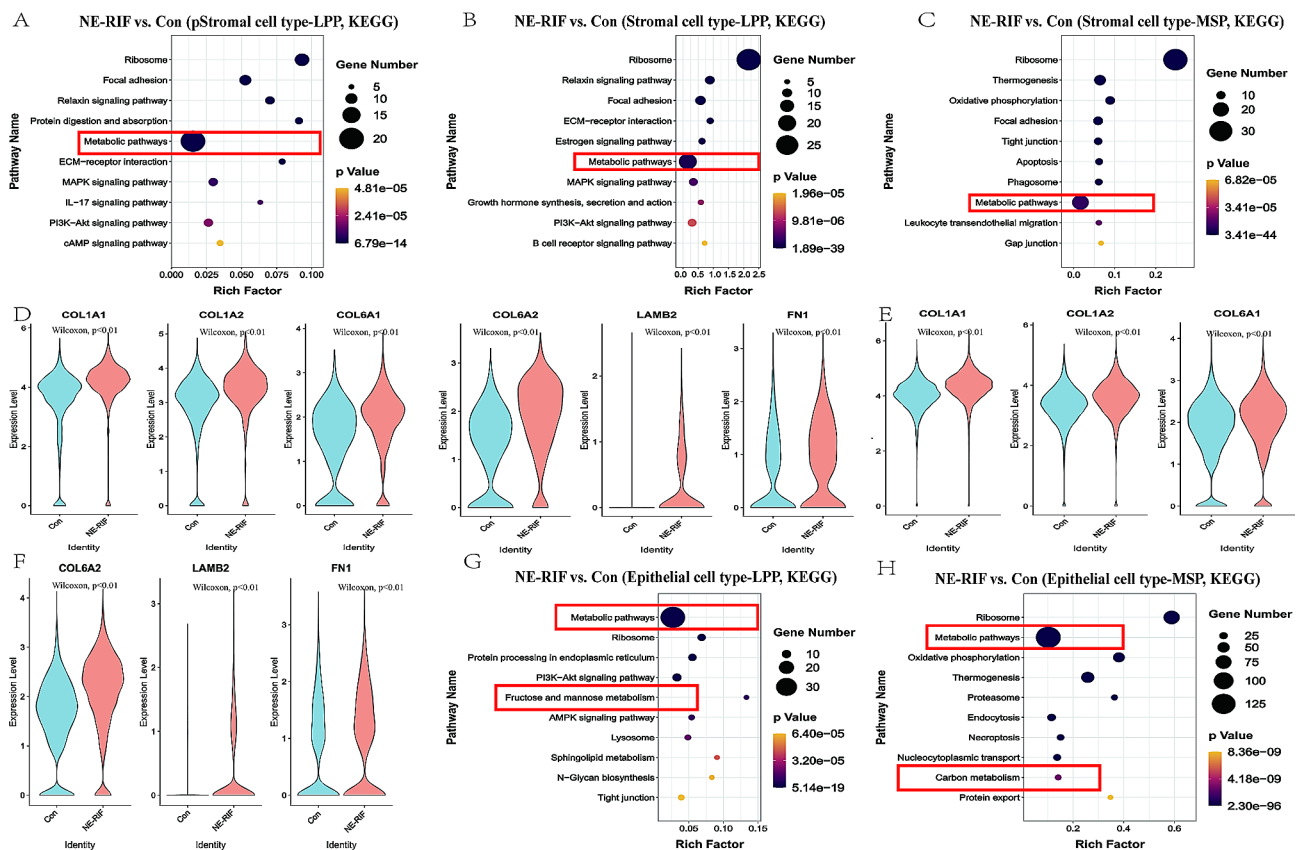


Fig. 7 Distribution of key transcription factors between NE-RIF patients and the control sample. **(A)** KEGG (Kyoto Encyclopedia of Genes and Genomes) enrichment analysis of the upregulated differentially expressed genes in pStromal cells between the NE-RIF and control groups during the late proliferative phase ($p < 0.01$, $\log FC < 0.26$ & $\log FC > -0.26$). **(B, C)** KEGG enrichment analysis of the upregulated differentially expressed genes in stromal cells between the NE-RIF and control groups during the late proliferative phase (B) and the mid-secretory phase (C) ($p < 0.01$, $\log FC < 0.26$ & $\log FC > -0.26$). **(D-F)** Violin plots showing the expression of collagen- and integrin-related genes in pStromal cells (D) and stromal cells (E, F) during the late proliferative phase; orange denotes NE-RIF patients, and blue denotes control volunteers. **(G)** KEGG enrichment analysis of the upregulated differentially expressed genes in epithelial cells between the NE-RIF and control groups during the late proliferative phase. **(H)** KEGG enrichment analysis during the mid-secretory phase ($p < 0.01$, $\log FC < 0.26$ & $\log FC > -0.26$). TE-RIF: recurrent implantation failure patients with thin endometrium, NE-RIF: recurrent implantation failure patients with normal endometrium thickness, control: fertile volunteers

cell cycle of pStromal cells was abnormal in both TE-RIF and NE-RIF groups, which could potentially impact the differentiation of stromal cells (Figs. 2E-J and 3A-E). In our previous study, the proportion of stromal cells increased and that of epithelial cells decreased in the control group in MSP, but the TE-RIF group showed the opposite pattern [11], as confirmed in this study. Additionally, we found that in the NE-RIF group, stromal cells failed to increase in MSP, while epithelial cells in this group decreased in MSP (Fig. 2E-J). Consistent with our earlier work, the estrogen receptor and progesterone receptor related to TE-RIF receptivity were downregulated in this study (Figs. 4A and 5B-D). Furthermore, our current investigation placed greater emphasis on understanding the intercellular communication dynamics between these two cell types, whereas our previous study suggested inadequate secretion of collagen and integrins in both stromal and epithelial cells.

Our findings also aligned with recent research indicating cell cycle dysfunction in pStromal and stromal cells. Specifically, the expression of PCNA, a proliferation marker, was found to be reduced in pStromal cells in the G1, S, and G2/M phases in thin endometrium [10]. Considering that stromal cells were differentiated from pStromal cells (Fig. 3F-H), we suspected that this dysfunction might extend to stromal cells, potentially shortening their survival cycle. This could contribute to the challenge of thickening thin endometrium. Moreover, these abnormal stromal cells might adversely affect endometrial receptivity. MAPK signaling pathways, highlighted in our study, have been reported to activate downstream inflammation factors and mediate cellular senescence through ROS by oxidative modification of kinases in the p38 MAPK signaling cascade (Fig. 3B) [37, 53, 54].

Endometrial epithelial cells play a crucial role in blastocyst apposition and adhesion. In LPP, epithelial cells responded to estrogen, forming the foundation for supportive and adhesive epithelial cells in MSP [7]. Therefore, the reduced expression of ESR1 (Fig. 5B) and downregulated estrogen signaling pathway (Fig. 5I) in the TE-RIF group suggested that the growth and differentiation of epithelial cells were inhibited. Additionally, the downregulation of the ECM-receptor signaling pathway indicated impaired nutrient provision and adhesion capacity for embryo implantation (Fig. 5A, F). In MSP, laminins and collagens were regulated by progesterone and accumulated in the endometrium [55, 56]. In line with this, a decrease in PGR expression in epithelial cells was observed in the TE-RIF group (Fig. 5E), and the downregulated ECM pathway in the TE-RIF group led to insufficient secretion of collagens, integrins, and laminins (Figs. 5F and 6F). This resulted in an abnormal endometrial structure during the secretory phase, failing to provide a conducive implantation environment for embryos.

In summary, compromised estrogen and progesterone function during the LPP and MSP in the TE-RIF group prevented epithelial cells from achieving a receptive state.

A study pointed out that co-culturing SFRP4+stromal cells with epithelial cells enhanced the growth of both cell types. A dynamic interaction between stromal and epithelial cells through WNT5A-SFRP4 in LPP was observed in our study (Fig. 6C) [9, 47]. While previous research has focused on stromal cells in TE-RIF, we suggest that epithelial-stromal cell interactions are also critical for endometrial growth and decidualization.

Conclusion

Our study sheds light on the distinct pathogenesis of TE-RIF and NE-RIF, employing scRNA-seq. Our findings underscore the significance of disrupted cell cycles and differentiation in pStromal cells, reveal intricate networks of communication between epithelial and stromal cells, and identify disordered carbohydrate and collagen metabolism, which contribute to challenges in endometrial receptivity. These findings may be harnessed to optimize individualized treatments for RIF patients.

Supplementary information

The online version contains supplementary material available at <https://doi.org/10.1186/s12958-024-01263-1>.

Supplementary Material 1

Acknowledgements

None.

Author contributions

Xiaoying Fu collected and analyzed the data, and was a major contributor to writing the manuscript. Xiaoyan Guo, Han Xu and Yini Li were responsible for revising the article and analyzing data. Han Xu collected clinical patients' data and processed the collected tissue. Bihui Jin, Xirong Zhang, Yuhang Fan, Yiqi Yu, Yuqing Tian collected clinical patients' data and processed the collected tissue. Chongyi Shu performed scanning and transmission electron microscopy. Jiao Tian supervised the writing of part of the article. Shu Jing was the initiator and organizer of the project. All authors read and approved the final manuscript.

Funding

This work was supported by the Co-construction Project from State and Zhejiang Administration of Traditional Chinese Medicine (GZY-ZJ-KJ-23058), and the General Research Program for Medicine and Health of Zhejiang Province (2023KY021,2022RC104).

Data availability

Raw single-cell RNA sequencing data can be accessed from the NCBI Gene Expression Omnibus database (BioProject ID: PRJNA1141235).

Declarations

Ethics approval and consent to participate

Zhejiang Provincial People's Hospital approved the use of human tissue for this study (2019QT003).

Consent for publication

All our participants signed the consent forms.

Competing interests

The authors declare no competing interests.

Author details

- ¹Center for Reproductive Medicine, Department of Reproductive Endocrinology, Affiliated People's Hospital, Zhejiang Provincial People's Hospital, Hangzhou Medical College, Hangzhou, Zhejiang, China
- ²Center for Reproductive Medicine, The First Affiliated Hospital, Zhejiang University School of Medicine, Hangzhou, China
- ³Zhejiang Provincial Key Laboratory of Pancreatic Disease, the First Affiliated Hospital, Zhejiang University School of Medicine, Hangzhou, China
- ⁴Shanghai First Maternity and Infant Hospital, School of Medicine, Tongji University, Shanghai, China
- ⁵The First Affiliated Hospital, Zhejiang University School of Medicine, 79 Qingchun Road, Shangcheng District, Hangzhou, Zhejiang, China

Received: 24 January 2024 / Accepted: 22 July 2024

Published online: 31 July 2024

References

- Inhorn MC, Patrizio P. Infertility around the globe: new thinking on gender, reproductive technologies and global movements in the 21st century. *Hum Reprod Update*. 2015;21:411–26.
- Pinborg A, Wennerholm UB, Bergh C. Long-term outcomes for children conceived by assisted reproductive technology. *Fertil Steril*. 2023;120:449–56.
- Ma J, Gao W, Li D. Recurrent implantation failure: a comprehensive summary from etiology to treatment. *Front Endocrinol (Lausanne)*. 2022;13:1061766.
- Thornhill AR, deDie-Smulders CE, Geraedts JP, Harper JC, Harton GL, Lavery SA, Moutou C, Robinson MD, Schmutzler AG, Scriven PN, et al. ESHRE PGD Consortium 'Best practice guidelines for clinical preimplantation genetic diagnosis (PGD) and preimplantation genetic screening (PGS)'. *Hum Reprod*. 2005;20:35–48.
- Liu KE, Hartman M, Hartman A. Management of thin endometrium in assisted reproduction: a clinical practice guideline from the Canadian fertility and Andrology Society. *Reprod Biomed Online*. 2019;39:49–62.
- Kasius A, Smit JG, Torrance HL, Eijkemans MJ, Mol BW, Opmeer BC, Broekmans FJ. Endometrial thickness and pregnancy rates after IVF: a systematic review and meta-analysis. *Hum Reprod Update*. 2014;20:530–41.
- Wang HQ, Liu Y, Li D, Liu JY, Jiang Y, He Y, Zhou JD, Wang ZL, Tang XY, Zhang Y et al. Maternal and embryonic signals cause functional differentiation of luminal epithelial cells and receptivity establishment. *Dev Cell* 2023.
- Lai ZZ, Wang Y, Zhou WJ, Liang Z, Shi JW, Yang HL, Xie F, Chen WD, Zhu R, Zhang C, et al. Single-cell transcriptome profiling of the human endometrium of patients with recurrent implantation failure. *Theranostics*. 2022;12:6527–47.
- Wu B, Li Y, Nie N, Shen X, Jiang W, Liu Y, Gong L, An C, Zhao K, Yao X, et al. SFRP4(+) stromal cell subpopulation with IGF1 signaling in human endometrial regeneration. *Cell Discov*. 2022;8:95.
- Lv H, Zhao G, Jiang P, Wang H, Wang Z, Yao S, Zhou Z, Wang L, Liu D, Deng W et al. Deciphering the endometrial niche of human thin endometrium at single-cell resolution. *Proc Natl Acad Sci U S A* 2022, 119.
- Zhang X, Li Y, Chen X, Jin B, Shu C, Ni W, Jiang Y, Zhang J, Ma L, Shu J. Single-cell transcriptome analysis uncovers the molecular and cellular characteristics of thin endometrium. *Faseb j*. 2022;36:e22193.
- Butler A, Hoffman P, Smibert P, Papalexi E, Satija R. Integrating single-cell transcriptomic data across different conditions, technologies, and species. *Nat Biotechnol*. 2018;36:411–20.
- McDavid A, Finak G, Chattopadhyay PK, Dominguez M, Lamoreaux L, Ma SS, Roederer M, Gottardo R. Data exploration, quality control and testing in single-cell qPCR-based gene expression experiments. *Bioinformatics*. 2013;29:461–7.
- Kanehisa M, Araki M, Goto S, Hattori M, Hirakawa M, Itoh M, Katayama T, Kawashima S, Okuda S, Tokimatsu T, Yamanishi Y. KEGG for linking genomes to life and the environment. *Nucleic Acids Res*. 2008;36:D480–484.
- Efremova M, Vento-Tormo M, Teichmann SA, Vento-Tormo R. CellPhoneDB: inferring cell-cell communication from combined expression of multi-subunit ligand-receptor complexes. *Nat Protoc*. 2020;15:1484–506.
- Hess A, Nayak N, Giudice L. Oviduct and EndometriumCyclic changes in the Primate Oviduct and Endometrium. *In*; 2006: 337–81.
- Nikas G. Pinopodes as markers of endometrial receptivity in clinical practice. *Hum Reprod*. 1999;14(Suppl 2):99–106.
- Czernobilsky B, Garcia CR, Wallach EE. Endometrial histology and parenteral estrogen-progestogen administration. *Fertil Steril*. 1969;20:75–90.
- Garry R, Hart R, Karthigasu KA, Burke C. A re-appraisal of the morphological changes within the endometrium during menstruation: a hysteroscopic, histological and scanning electron microscopic study. *Hum Reprod*. 2009;24:1393–401.
- Halari CD, Nandi P, Jeyarajah MJ, Renaud SJ, Lala PK. Decrin production by the human decidua: role in decidual cell maturation. *Mol Hum Reprod*. 2020;26:784–96.
- Xu L, Fan Y, Wang J, Shi R. Dysfunctional intercellular communication and metabolic signaling pathways in thin endometrium. *Front Physiol*. 2022;13:1050690.
- Wang W, Vilella F, Alama P, Moreno I, Mignardi M, Isakova A, Pan W, Simon C, Quake SR. Single-cell transcriptomic atlas of the human endometrium during the menstrual cycle. *Nat Med*. 2020;26:1644–53.
- Bassez A, Vos H, Van Dyck L, Floris G, Arijis I, Desmedt C, Boeckx B, Vanden Bempt M, Nevelsteen I, Lambein K, et al. A single-cell map of intratumoral changes during anti-PD1 treatment of patients with breast cancer. *Nat Med*. 2021;27:820–32.
- Chen P, Zhou L, Chen J, Lu Y, Cao C, Lv S, Wei Z, Wang L, Chen J, Hu X, et al. The Immune Atlas of Human Deciduas with unexplained recurrent pregnancy loss. *Front Immunol*. 2021;12:689019.
- Hasegawa SL, Boss JM. Two B cell factors bind the HLA-DRA X box region and recognize different subsets of HLA class II promoters. *Nucleic Acids Res*. 1991;19:6269–76.
- David K, Friedlander G, Pellegrino B, Radomir L, Lewinsky H, Leng L, Bucala R, Becker-Herman S, Shachar I. CD74 as a regulator of transcription in normal B cells. *Cell Rep*. 2022;41:111572.
- Young MD, Mitchell TJ, Vieira Braga FA, Tran MGB, Stewart BJ, Ferdinand JR, Collord G, Botting RA, Popescu DM, Loudon KW, et al. Single-cell transcriptomes from human kidneys reveal the cellular identity of renal tumors. *Science*. 2018;361:594–9.
- Gerdes J, Schwab U, Lemke H, Stein H. Production of a mouse monoclonal antibody reactive with a human nuclear antigen associated with cell proliferation. *Int J Cancer*. 1983;31:13–20.
- Scholzen T, Gerdes J. The Ki-67 protein: from the known and the unknown. *J Cell Physiol*. 2000;182:311–22.
- Gerdes J, Li L, Schlueter C, Duchrow M, Wohlenberg C, Gerlach C, Stahmer I, Kloth S, Brandt E, Flad HD. Immunobiochemical and molecular biologic characterization of the cell proliferation-associated nuclear antigen that is defined by monoclonal antibody Ki-67. *Am J Pathol*. 1991;138:867–73.
- Shaulian E, Karin M. AP-1 as a regulator of cell life and death. *Nat Cell Biol*. 2002;4:E131–136.
- Okada S, Fukuda T, Inada K, Tokuhisa T. Prolonged expression of c-fos suppresses cell cycle entry of dormant hematopoietic stem cells. *Blood*. 1999;93:816–25.
- Yu M, Du G, Xu Q, Huang Z, Huang X, Qin Y, Han L, Fan Y, Zhang Y, Han X, et al. Integrated analysis of DNA methylome and transcriptome identified CREB5 as a novel risk gene contributing to recurrent pregnancy loss. *EBioMedicine*. 2018;35:334–44.
- Chhabra JK, Chattopadhyay B, Paul BN. SOCS3 dictates the transition of divergent time-phased events in granulocyte TNF-alpha signaling. *Cell Mol Immunol*. 2014;11:105–6.
- Rawlings TM, Makwana K, Taylor DM, Molè MA, Fishwick KJ, Tryfonos M, Odendaal J, Hawkes A, Zernicka-Goetz M, Hartshorne GM et al. Modelling the impact of decidual senescence on embryo implantation in human endometrial assembloids. *Elife* 2021, 10.
- Diaz-Gimeno P, Horcajadas JA, Martinez-Conejero JA, Esteban FJ, Alama P, Pellicer A, Simon C. A genomic diagnostic tool for human endometrial receptivity based on the transcriptomic signature. *Fertil Steril*. 2011;95:50–60. 60 e51–15.
- Tong M, Kayani T, Jones DM, Salmon JE, Whirledge S, Chamley LW, Abrahams VM. Antiphospholipid antibodies increase endometrial stromal cell decidualization, senescence, and inflammation via toll-like receptor 4, reactive oxygen species, and p38 MAPK signaling. *Arthritis Rheumatol*. 2022;74:1001–12.
- Tang Y, Qiu J, Tang Z, Li G, Gu M, Wang Y, Bao H, Deng W, Lu Z, Otsu K, et al. P38alpha MAPK is a gatekeeper of uterine progesterone responsiveness at peri-implantation via Ube3c-mediated PGR degradation. *Proc Natl Acad Sci U S A*. 2022;119:e2206000119.

39. Lavoie H, Gagnon J, Therrien M. ERK signalling: a master regulator of cell behaviour, life and fate. *Nat Rev Mol Cell Biol.* 2020;21:607–32.
40. Cha J, Sun X, Dey SK. Mechanisms of implantation: strategies for successful pregnancy. *Nat Med.* 2012;18:1754–67.
41. Pavlik EJ, Katzenellenbogen BS. Human endometrial cells in primary tissue culture: estrogen interactions and modulation of cell proliferation. *J Clin Endocrinol Metab.* 1978;47:333–44.
42. Gebril M, Hirota Y, Aikawa S, Fukui Y, Kaku T, Matsuo M, Hirata T, Akaeda S, Hiraoka T, Shimizu-Hirota R et al. Uterine epithelial progesterone receptor governs uterine receptivity through epithelial cell differentiation. *Endocrinology* 2020, 161.
43. Fitzgerald HC, Dhakal P, Behura SK, Schust DJ, Spencer TE. Self-renewing endometrial epithelial organoids of the human uterus. *Proc Natl Acad Sci U S A.* 2019;116:23132–42.
44. Burton GJ, Jauniaux E, Charnock-Jones DS. Human early placental development: potential roles of the endometrial glands. *Placenta.* 2007;28(Suppl A):S64–69.
45. Tempest N, Jansen M, Baker AM, Hill CJ, Hale M, Magee D, Treanor D, Wright NA, Hapangama DK. Histological 3D reconstruction and in vivo lineage tracing of the human endometrium. *J Pathol.* 2020;251:440–51.
46. Hernández-Vargas P, Muñoz M, Domínguez F. Identifying biomarkers for predicting successful embryo implantation: applying single to multi-OMICS to improve reproductive outcomes. *Hum Reprod Update.* 2020;26:264–301.
47. Tribulo P, Siqueira LGB, Oliveira LJ, Scheffler T, Hansen PJ. Identification of potential embryokines in the bovine reproductive tract. *J Dairy Sci.* 2018;101:690–704.
48. Kelleher AM, DeMayo FJ, Spencer TE. Uterine glands: Developmental Biology and functional roles in pregnancy. *Endocr Rev.* 2019;40:1424–45.
49. Kim TH, Yoo JY, Choi KC, Shin JH, Leach RE, Fazleabas AT, Young SL, Lessey BA, Yoon HG, Jeong JW. Loss of HDAC3 results in nonreceptive endometrium and female infertility. *Sci Transl Med* 2019, 11.
50. Rahima A, Soderwall AL. Uterine collagen content in young and senescent pregnant golden hamsters. *J Reprod Fertil.* 1977;49:161–2.
51. Bermejo-Alvarez P, Roberts RM, Rosenfeld CS. Effect of glucose concentration during in vitro culture of mouse embryos on development to blastocyst, success of embryo transfer, and litter sex ratio. *Mol Reprod Dev.* 2012;79:329–36.
52. Diamond MP, Pettway ZY, Logan J, Moley K, Vaughn W, DeCherney AH. Dose-response effects of glucose, insulin, and glucagon on mouse pre-embryo development. *Metabolism.* 1991;40:566–70.
53. Xu Y, Li N, Xiang R, Sun P. Emerging roles of the p38 MAPK and PI3K/AKT/mTOR pathways in oncogene-induced senescence. *Trends Biochem Sci.* 2014;39:268–76.
54. Borodkina A, Shatrova A, Abushik P, Nikolsky N, Burova E. Interaction between ROS dependent DNA damage, mitochondria and p38 MAPK underlies senescence of human adult stem cells. *Aging.* 2014;6:481–95.
55. Bulletti C, Galassi A, Jasonni VM, Martinelli G, Tabanelli S, Flamigni C. Basement membrane components in normal hyperplastic and neoplastic endometrium. *Cancer.* 1988;62:142–9.
56. Bilalis DA, Klentzeris LD, Fleming S. Immunohistochemical localization of extracellular matrix proteins in luteal phase endometrium of fertile and infertile patients. *Hum Reprod.* 1996;11:2713–8.

Publisher's Note

Springer Nature remains neutral with regard to jurisdictional claims in published maps and institutional affiliations.